# A new, fully ab initio investigation of the NO (X 2 Π) Ar system. I. Potential energy surfaces and inelastic scattering

Millard H. Alexander

Citation: The Journal of Chemical Physics **111**, 7426 (1999); doi: 10.1063/1.480066
View online: http://dx.doi.org/10.1063/1.480066
View Table of Contents: http://scitation.aip.org/content/aip/journal/jcp/111/16?ver=pdfcov
Published by the AIP Publishing

# A new, fully *ab initio* investigation of the NO($X\ ^2\Pi$)Ar system. I. Potential energy surfaces and inelastic scattering

Millard H. Alexander
*Department of Chemistry and Biochemistry, University of Maryland, College Park, Maryland 20742-2021*

(Received 30 April 1999; accepted 13 July 1999)

We report new coupled-cluster [CCSD(T)] *ab initio* calculations of the two potential energy surfaces (PES's) of the Ar–NO complex. Successively larger basis sets are used to extrapolate to the complete basis set limit. Although qualitatively very similar to our earlier PES's [M. H. Alexander, J. Chem. Phys. **99**, 7725 (1993)], the new PES's have substantially deeper wells ($D_e = 116\,\mathrm{cm}^{-1}$). Full close-coupled integral inelastic cross sections were determined at collision energies of 442 and 1774 $\mathrm{cm}^{-1}$ for transitions out of the lowest NO rotational level ($j=\omega=1/2$). For transitions into higher rotational levels of the same spin–orbit manifold the cross sections are little changed from previously calculated values, and still in some disagreement with recent experiments. For transitions in which the spin–orbit manifold changes ($\omega=1/2\rightarrow 3/2$), the calculated integral cross sections are larger than the previously calculated values at $E=442\,\mathrm{cm}^{-1}$ but agree quite closely at $E=1774\,\mathrm{cm}^{-1}$. At both energies, however, the calculated cross sections for spin–orbit changing transitions are noticeably smaller than experimentally derived values. © *1999 American Institute of Physics.* [S0021-9606(99)30138-0]

## I. INTRODUCTION

Collisions of molecular free radicals underlie all of chemical kinetics. These processes are complicated by the presence of electronic spin and/or orbital angular momentum, which can couple with the orbital angular momentum of the collision partners.[1] For systems with nonzero electronic orbital angular momentum, more than one potential energy surface (PES) is accessed during the collision. Consequently, the complete description of collisions involving free radicals is inherently quantum mechanical. From a semiclassical viewpoint the underlying collision ''trajectories'' evolve simultaneously and coherently on the coupled PES's.[2]

As in other areas of physical chemistry, the greatest progress in the understanding of molecular reaction dynamics involving open-shell species comes from the detailed investigation of exemplary systems, which are simultaneously tractable by both theoreticians and experimentalists. For inelastic scattering, collisions of noble gasses with NO have emerged as the paradigm.[3] Experimental interest goes back nearly two decades[4,5] and continues unabated to this day.[1,6–9]

Several early papers[10–13] set the theoretical framework for the understanding of inelastic collisions involving molecules in $\Pi$ electronic states. Because of the spatial anisotropy of the electronic wave function, two PES's are required to describe the interaction between a diatomic in a $\Pi$ electronic and a spherical target.[13] Pack and co-workers used density functional methods to determine the two PES's for the Ar–NO($X$) system.[14] We subsequently published more accurate, *ab initio* PES's,[15] determined using the correlated electron pair (CEPA) method.[16,17] These have been used in a number of theoretical determinations of integral[8,15,18–20] and differential[15,20] cross sections for the scattering of NO($X$) by Ar as well as the bound states of the ArNO complex.[21]

In almost all of the prior experimental scattering studies, both $\Lambda$-doublet (parity) levels of the lowest ($j=\omega=1/2$) rotational, spin–orbit level of NO were present initially. In recent work Stolte and co-workers have used an electric hexapole to prepare beams of NO($X$) solely in the upper $\Lambda$-doublet level.[7] These authors then determined integral cross sections for scattering out of this single $\Lambda$-doublet state into higher rotational levels of the $\omega=1/2$ spin–orbit manifold at a collision energy of 442 $\mathrm{cm}^{-1}$, nearly identical to the collision energy in the pioneering experiments of Andersen and co-workers.[5,22] Scattering of this single state reveals[7,15] a greater degree of structure in the final state distribution. Comparison between the theoretically calculated cross sections and those determined by Stolte and co-workers[7] shows some disagreement: theory predicts a larger degree of inelasticity (larger cross sections for large $\Delta j$ transitions) than is seen experimentally.

The cross sections for transitions in which the spin–orbit manifold changes, the calculated cross sections, based on our CEPA PES's, are considerably smaller than those observed experimentally,[15] both by Andresen *et al.*[5,22] at a collision energy of 442 $\mathrm{cm}^{-1}$ and by McBane and co-workers[9] at a collision energy of 1774 $\mathrm{cm}^{-1}$ (220 meV).

In an attempt to ascertain whether the remaining discrepancies with experiment are due to inadequacies in the ArNO PES's, we present here new calculations, based on a coupled-cluster [CCSD(T)][23] treatment with a larger atomic orbital basis set than used previously.[15] As will be seen below, the agreement with the collision experiments is little improved.

## II. POTENTIAL ENERGY SURFACES

The approach of a structureless atom to a molecule in a $^2\Pi$ electronic state gives rise to two PES's, of $A''$ and $A'$ symmetry with respect to reflection in the triatomic plane.[13]

 

The PES's are a function of the three Jacobi coordinates used to describe the triatomic system: $r$ (the NO bond distance), $R$ (the distance between the Ar atom and the center of mass of the NO molecule) and $\theta$ (the angle between $r$ and $R$). In our previous investigation of the ArNO system, we used the CEPA method[16,17,24] and the augmented, triple-zeta, correlation consistent (*avtz*) atomic orbital bases of Dunning and co-workers.[25–27] The NO bond distance was held fixed at its equilibrium value [1.5077 Å (Ref. 28)].

In the present investigation we carried out unrestricted coupled-cluster (singles and doubles) with the perturbative inclusion of triple excitations [UCCSD(T)].[23] Calculations were done with double-, triple-, and quadruple-zeta, correlation consistent basis sets (*avdz*, *avtz*, and *avqz*), in each case augmented with additional diffuse functions to describe more accurately the electronic correlation in the weakly bound complex.[25–27] Calculations were carried out for 11 values of $R$ [4.5:0.5:8, 9, 10, 12] and 9 values of $\theta$ [0, 30, 60, 75, 90, 105, 120, 150, and 180°].

The interaction energy for each orientation and for each electronic state ($A'$ or $A''$) is given by

$$V(R,\theta)=E_{\mathrm{ArNO}}(R,\theta)-E_{\mathrm{NO}}(\infty)-E_{\mathrm{Ar}}(\infty)-\Delta E_{\mathrm{CP}}(R,\theta). \tag{1a}$$

Here, the counterpoise correction,[29] which adjusts for the lack of saturation of the orbital basis, is defined by

$$\Delta E_{\mathrm{CP}}(R,\theta)=E_{\mathrm{NO}}(R,\theta)+E_{\mathrm{Ar}}(R,\theta)-E_{\mathrm{NO}}(\infty)-E_{\mathrm{Ar}}(\infty). \tag{1b}$$

Since the lowest energy configuration of the ArNO complex is thought to lie near perpendicular geometries,[15,21,30] a finer angular grid (15°) was used in this region. Exploratory calculations with the *avtz* basis were carried out including the missing angles on a 15° grid (15, 45, 135, and 165°). The interpolated dependence on $\theta$ of the PES's differed imperceptibly from that obtained from the 9 original angles.

Additionally, in the region of the minimum, further calculations with the *avtz* basis were carried out in which we allowed the NO bond distance to vary. The relative $r$ dependence of the calculated PES's differed imperceptibly from that determined with the same basis set and the Ar atom located at a large distance. This justifies the use of a fixed NO bond distance in the calculation of the PES's.

At each of the 99 points, we extrapolated the *avdz*, *avtz*, and *avqz* interaction energies to the complete basis set (CBS) limit, by means of the expression[31]

$$V_n=V_\infty+A\exp(n-1)+B\exp[(n-1)^2], \tag{2}$$

where $n=2$ for *avdz*, $n=3$ for *avtz*, and $n=4$ for *avqz*.

In the treatment of the nuclear motion of the complex, it is convenient to work with the average and half-difference of the PES's for the states of $A''$ and $A'$ reflection symmetry, which we define as[13]

$$V_{\mathrm{sum}}(R,\theta)=0.5[V_{A''}(R,\theta)+V_{A'}(R,\theta)] \tag{3a}$$

and

$$V_{\mathrm{dif}}(R,\theta)=0.5[V_{A''}(R,\theta)-V_{A'}(R,\theta)] \tag{3b}$$

The dependence on $\theta$ is then expanded[13] in reduced rotation matrix elements,[32]

TABLE I. Minimum geometry and energy of Ar–NO ($X$) complex.[a]

| | CEPA[b] | CCSD(T) | | |
|---|---|---|---|---|
| | *avtz* | *avtz* | *avqz* | CBS limit[c] |
| $R_e(A')$ | 6.99 | 6.90 | 6.81 | 6.76 |
| $R_e(A'')$ | 7.09 | 7.09 | 6.97 | 6.92 |
| $\theta_e(A')$ | 94.1 | 95.2 | 95.0 | 94.9 |
| $\theta_e(A'')$ | 73.1 | 69.7 | 70.1 | 69.9 |
| $D_e(A')$ | 77.9 | 95.5 | 108.1 | 115.9 |
| $D_e(A'')$ | 79.1 | 92.1 | 103.6 | 111.0 |

[a]Distances in bohr, angles in degrees, energy in $\mathrm{cm}^{-1}$.
[b]Reference 15.
[c]Complete basis set limit; Eq. (2), where $n=2$, 3, and 4 for *avdz*, *avtz*, and *avqz*, respectively.

$$V_{\mathrm{sum}}(R,\theta)=\sum_{\lambda=0}^{\lambda_{\max}} V_{\lambda 0}(R)d_{00}^{\lambda}(\theta) \tag{4a}$$

and

$$V_{\mathrm{dif}}(R,\theta)=\sum_{\lambda=2}^{\lambda_{\max}} V_{\lambda 2}(R)d_{20}^{\lambda}(\theta), \tag{4b}$$

where $\lambda_{\max}=9$, corresponding to the number of angles in the *ab initio* grid.

To determine the expansion coefficients $V_{\lambda 2}(R)$ and $V_{\lambda 0}(R)$ for any value of $R$ and $\theta$, we first fit the *ab initio* CBS interaction energies $V_{A'}(R_i,\theta_j)$ and $V_{A''}(R_i,\theta_j)$, for each value of $\theta_i$ separately, to the general functional form[33]

$$V(R,\theta_i)=c_{1i}\exp(-b_{1i}R)+(c_{2i}+c_{3i}R)\exp(-b_{2i}R)+c_{4i}\{\tanh[1.2(R-R_{0i})]-1\}/R^6. \tag{5}$$

The linear and nonlinear parameters were adjusted to minimize the relative deviation of all points with $V\leqslant 7000\ \mathrm{cm}^{-1}$. The rms relative and absolute errors in the fit to all the *ab initio* points were, respectively, 0.002 and 0.29 $\mathrm{cm}^{-1}$.

Then, for any value of $R$, the expansion parameters in Eq. (5) are used to determine $V(R,\theta_i)$ at the 9 angles, and the $V_{\lambda 2}(R)$ and $V_{\lambda 0}(R)$ coefficients obtained by solution of a set of linear equations.

Table I compares the location and depths of the minima on the $A'$ and $A''$PES's with the results of our previous CEPA calculations. As can be seen, the CCSD(T) minima are substantially deeper and located at slightly smaller values of $R$. This is consistent with a more complete recovery of the correlation energy, which is responsible for the dispersion energy which provides the bonding. The minima on the $A'$ and $A''$PES's occur at somewhat different geometries, but are very similar in depth. It is significant that the CCSD(T) calculations consistently predict the well on the $A'$PES to be slightly lower, in contrast to the CEPA calculations.

Figures 1–4 compare contour plots of the CEPA and CCSD(T) $A'$ and $A''$ PES. As can be seen, the topology of the CEPA and CCSD(T) PES's are globally extremely similar, despite the significantly deeper wells in the latter PES's.

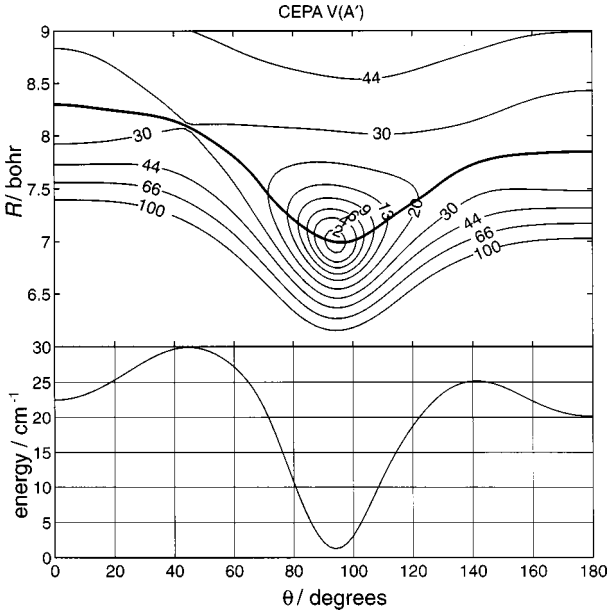


FIG. 1. (Upper panel) Contour plot of the PES of the ArNO state of $A'$ reflection symmetry, as predicted by our earlier CEPA calculations (Ref. 15). The energies are in $cm^{-1}$, with respect to the minimum of the potential ($D_e = 77.9\ cm^{-1}$; see Table I). The heavy curve indicates the minimum of the PES as a function of $\theta$, the relative energy along this heavy curve is indicated in the lower panel.

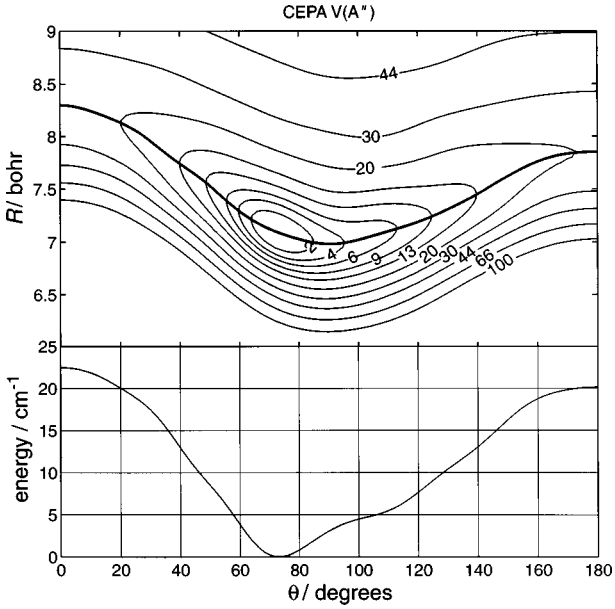


FIG. 3. (Upper panel) Contour plot of the PES of the ArNO state of $A''$ reflection symmetry, as predicted by our earlier CEPA calculations (Ref. 15). The energies are in $cm^{-1}$, with respect to the minimum of the potential ($D_e = 79.1\ cm^{-1}$; see Table I). The heavy curve indicates the minimum of the PES as a function of $\theta$, the relative energy along this heavy curve is indicated in the lower panel.

Figure 5 shows contour plots for the CCSD(T) sum potential, $V_{\rm sum}$ while Fig. 6 compares the CEPA and CCSD(T) difference potentials, $V_{\rm dif}$. As can be seen, the difference potentials are very similar.

## III. SCATTERING OF NO BY AR: FORMALISM

To describe the rotational levels of the NO($X$) molecule in its $^2\Pi$ electronic state we use a Hund's case (a) basis:[34]

$$|\lambda\sigma jm\omega\varepsilon\rangle = 2^{-1/2}[|jm\omega\rangle|\lambda\sigma\rangle + \varepsilon|jm-\omega\rangle|-\lambda-\sigma\rangle]. \tag{6}$$

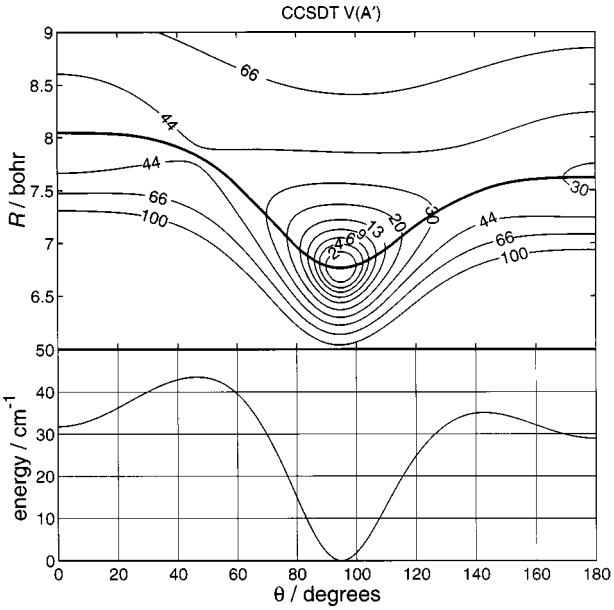


FIG. 2. (Upper panel) Contour plot of the PES of the ArNO state of $A'$ reflection symmetry, as predicted by the present CCSD(T) calculations, extrapolated to the complete basis set limit. The energies are in $cm^{-1}$, with respect to the minimum of the potential ($D_e = 115.9\ cm^{-1}$; see Table I). The heavy curve indicates the minimum of the PES as a function of $\theta$; the relative energy along this heavy curve is indicated in the lower panel.

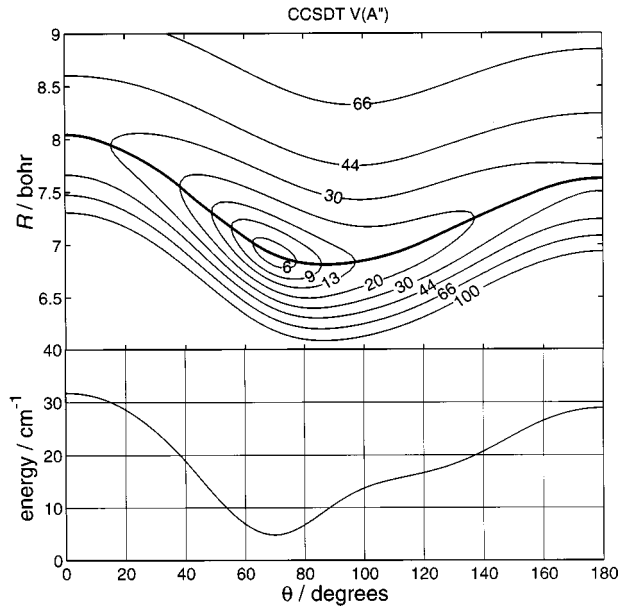


FIG. 4. (Upper panel) Contour plot of the PES of the ArNO state of $A''$ reflection symmetry, as predicted by the present CCSD(T) calculations, extrapolated to the complete basis set limit. The energies are in $cm^{-1}$, with respect to the minimum of the potential ($D_e = 111.0\ cm^{-1}$; see Table I). The heavy curve indicates the minimum of the PES as a function of $\theta$; the relative energy along this heavy curve is indicated in the lower panel.

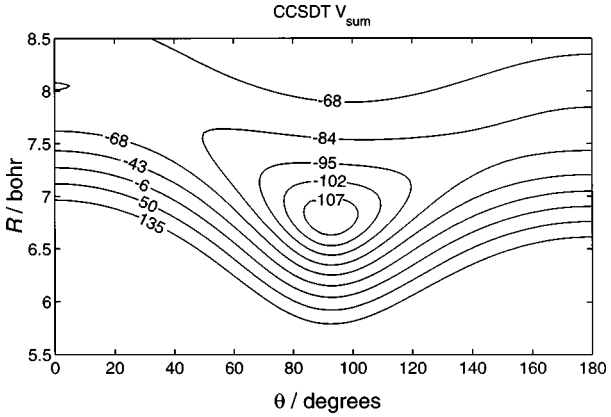


FIG. 5. Contour plot of the average ($V_{\rm sum}$) ArNO PES from the present CCSD(T) calculations, extrapolated to the complete basis set limit. The energies are in $\rm cm^{-1}$. The minimum is $-109.8$ $\rm cm^{-1}$.

Here $j$ denotes the total angular momentum of the diatomic molecule, with projections $m$ and λ along, respectively, the space- and molecule-fixed $z$-axes. Also $|\lambda\sigma\rangle$ designates the electronic component of the wave function where λ and $\sigma$ denote, respectively, the molecule-frame projections of the electronic orbital and spin angular momenta. The Λ- (or ''parity'') doublet levels are distinguished by the symmetry index $\varepsilon$ which can take the value $+1$ ($e$-labeled levels) or $-1$ ($f$-labeled levels).[35] The total parity of the wave functions is given by $\varepsilon(-1)^{j-1/2}$.[35] For simplicity in what follows, we will suppress the electronic wave function $|\lambda\sigma\rangle$ and the λ and $\sigma$ quantum numbers, except when needed. Our use here of lower case letters to designate the quantum numbers of the diatomic moiety is consistent with the notation of Dubernet *et al.*[36] and Green and Lester[37] and is used for historical continuity in the discussion of the bound states of the Ar–NO complex, which is described in the accompanying paper.[38]

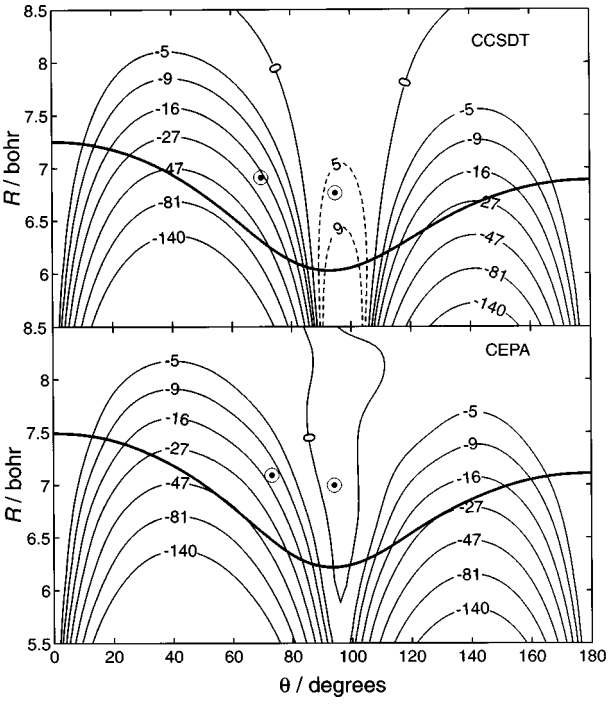


FIG. 6. (Upper panel) Contour plot of the difference ($V_{\rm dif}$) ArNO PES from the present CCSD(T) calculations, extrapolated to the complete basis set limit. The energies are in $\rm cm^{-1}$. The heavy curve indicates the edge of the repulsive wall on the CCSD(T) $V_{\rm sum}$ PES (Fig. 5). The two circles indicate the position of the minima on the $A'$ and $A''$ CCSD(T) PES's (see Figs. 2 and 4). (Lower panel) Similar contour plot of $V_{\rm dif}$ from our earlier CEPA calculations (Ref. 15).

The $j\cdot s$ term in the molecular Hamiltonian[34] mixes the $\omega=1/2$ and $\omega=3/2$ case (a) basis functions. The mixed diatomic wave functions can be expressed as linear combinations of the definite $\omega$ functions of Eq. (6), namely,

$$|jmF_i\epsilon\rangle=\sum_{\omega} D^{j}_{F_i\omega\varepsilon}|jm\omega\varepsilon\rangle. \tag{7}$$

The expansion coefficients $D^{j}_{F_i\omega\varepsilon}$ are obtained by diagonalization of the Hamiltonian of the isolated NO molecule.[34,39,40] The mixed states are denoted $F_1$ and $F_2$ in terms of increasing energy.[41] For the NO molecule, where the spin–orbit splitting is much larger than the rotational constant, the mixing is small at low $j$, so that $\omega$ is a nearly good quantum number. For the NO molecule the $\omega=1/2$ spin–orbit manifold lies lower in energy, so that the lowest rotational state is $j=\omega=1/2$. In addition, the $f$ Λ-doublet levels lie slightly ($\sim$0.01 $\rm cm^{-1}$) higher in energy

The complete wave function for the ArNO system is expanded as

$$\Psi^{JM}=(1/R)\sum_{jLF_i\varepsilon} C^{JM}_{jLF_i\varepsilon}(R)|jF_i\varepsilon LJM\rangle, \tag{8}$$

where $J$ is the total angular momentum. Here, the $|jF_i\varepsilon LJM\rangle$ functions are composed of products of the NO electronic-rotation functions $|jmF_i\varepsilon\rangle$ [Eq. (7)] and angular momentum functions which describe the orbital (end-over-end) rotation of the ArNO complex ($L=J-j$), namely

$$|jF_i\varepsilon LJM\rangle=\sum_{mM_L}(jmLM_L|JM)Y_{LM_L}(\hat{R})|jmF_i\varepsilon\rangle, \tag{9}$$

where $Y_{LM_L}(\hat{R})$ is a spherical harmonic and $(\cdots|\cdots)$ is a Clebsch–Gordon coefficient.[42] Each state included in the expansion of Eq. (8) defines a ''channel.''

The expansion coefficients, $C^{JM}_{jLF_i\varepsilon}$, in Eq. (8) are independent of $M$ and satisfy the standard close-coupled (CC) equations. In matrix notation these are

$$\left(\frac{d^2}{dR^2}+W(R)\right)C^{J}(R)=0, \tag{10}$$

where

$$W(R)\equiv k^2-\frac{L^2}{R^2}-\frac{2\mu}{\hbar^2}V(R). \tag{11}$$

Here $k^2$ designates the diagonal matrix containing the wave vectors of the individual coupled channels, and $L^2$ and $V(R)$ are the full matrices of, respectively, the square of the orbital angular momentum $L$ and the interaction potential(s). The matrix elements of the interaction potential for a $^2\Pi$ system in the intermediate coupling basis of Eq. (9) have been given previously.[13,43]

## IV. SCATTERING CALCULATIONS: RESULTS

Close-coupled[12,13,43] scattering calculations were carried out for the Ar–NO system at a total energy ($E_{\rm tot}$) of 442 $\rm cm^{-1}$ (0.0548 eV). We take the lowest rotational state of NO ($j=\omega=1/2$), to define the zero of energy, so that $E_{\rm tot}=442\,\rm cm^{-1}$ corresponds to an initial collision energy of 442 $\rm cm^{-1}$ for the scattering of NO in the $j=\omega=1/2$ level. This is the collision energy used in the recent experiments of Stolte and co-workers[7] as well as in the groundbreaking experiments of Andresen.[5,22] Similar calculations were also carried out at $E_{\rm tot}=1774\,\rm cm^{-1}$, the energy used in the recent experimental investigation of McBane and co-workers. The size of the state expansion in Eq. (8) (number of channels), as well as the integration parameters and maximum value of the total angular momentum $J$, were chosen[15,20] to ensure an accuracy of better than 1% in the calculated probabilities for all transitions out of the lowest rotational state of NO ($j=\omega=1/2$) into all higher levels with $j'\leqslant 25.5$. All scattering calculations were based on the formalism we have developed,[12,13,43] and performed with our Hibridon code.[44]

The asymptotic dependence of the $C^{JM}_{jLF_i\varepsilon}$ coefficients in Eq. (8) defines the fundamental scattering $S$ matrix. Integral cross sections for a collision-induced transition between initial and final electronic–rotational terms of the NO molecule $(j,\omega,\varepsilon\rightarrow j',\omega',\varepsilon')$, averaged over all values of the rotational projection quantum numbers can be obtained from the corresponding $S$-matrix elements.[12,13,43] The experiments of van Leuken *et al.*[7] probe directly the $\sigma(j\omega\varepsilon\rightarrow j'\omega'\varepsilon';E)$ cross sections.

In experiments such as those of Andresen and co-workers,[5,22] in which the initial $\Lambda$-doublet level is not selected (but assumed to be equally populated) and in which both final $\Lambda$-doublets are either detected or presumed to be equally populated, the appropriate cross section can be written as

$$\sigma(j\omega\rightarrow j'\omega';E)=\frac{1}{2}\sum_{\varepsilon,\varepsilon'}\sigma(j\omega,\varepsilon\rightarrow j'\omega'\varepsilon';E). \qquad (12)$$

The factor of 1/2 on the right-hand side of Eq. (12) reflects that assumption that the initial population is split equally between the two $\Lambda$-doublet states.

Finally, in experiments such as those of McBane and co-workers,[9] in which the initial $\Lambda$-doublet level is not selected (but assumed to be equally populated) and in which each final $\Lambda$-doublet is detected separately, the appropriate cross section can be written as

$$\sigma(j\omega\rightarrow j'\omega'\varepsilon';E)=\sigma(j\omega,\varepsilon=+1\rightarrow j'\omega'\varepsilon';E)+\sigma(j\omega,\varepsilon=-1\rightarrow j'\omega'\varepsilon';E). \qquad (13)$$

To be consistent with the earlier work of McBane and co-workers [see Eqs. (7) and (8) of Ref. 9] we have *not* included a factor of 1/2 in the right-hand side of Eq. (13), as was included in Eq. (12).

Figure 7 compares the CCSD(T) and CEPA degeneracy-averaged integral cross sections at $E_{\rm tot}=442\,\rm cm^{-1}$, summed and averaged over $\Lambda$-doublet level. The cross sections for transitions within the same spin–orbit manifold are virtually identical, except for the lowest two values of $j'$. For transitions in which the spin-orbit manifold changes (lower panel of Fig. 7), the CCSD(T) PES's predict significantly larger cross sections. For a molecule which is nearly Hund's case (a) at low $j$, transitions between different spin–orbit manifolds are induced by the difference potential, $V_{\rm dif}$, while $V_{\rm sum}$ controls the overall scattering.[12] As can be seen in Fig. 6, the CCSD(T) $V_{\rm dif}$ is slightly larger at the turning point of $V_{\rm sum}$ than the CEPA $V_{\rm dif}$. Consequently, we expect, and see, slightly enhanced cross sections for the spin-orbit changing transitions.

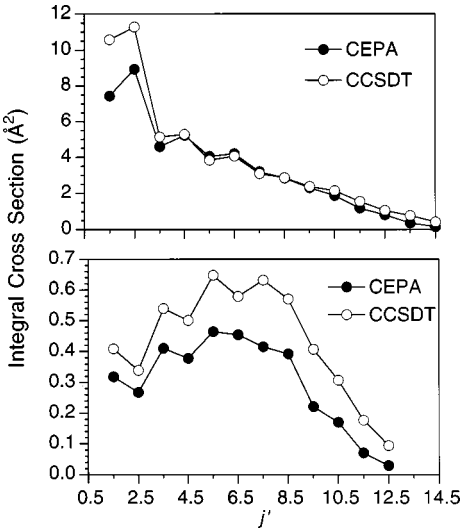


FIG. 7. Comparison of close-coupled, integral cross sections, averaged over initial and summed over final $\Lambda$-doublet level [Eq. (12)], for excitation out of the $j=\omega=1/2$ level of NO by collision with Ar; $E_{\rm tot}=442\,\rm cm^{-1}$. The filled and empty circles represent, respectively, predictions based on our earlier CEPA PES's (Ref. 15) and those based on the present CCSD(T) PES's. The upper and lower panels represents, respectively, excitation into rotational levels of the $\omega=1/2(F_1)$ and $\omega=3/2(F_2)$ spin–orbit manifolds.

Figure 8 presents a comparison of the CCSD(T) integral cross sections at 442 $\rm cm^{-1}$ with the experimental results of Joswig *et al.*[22] Since the experiment does not yield absolute cross sections, we have scaled both the experimental spin–orbit conserving and spin–orbit changing cross sections so that the sum of the former is equal to the sum of the CCSD(T) integral cross sections for the same transitions. As can be seen the agreement is excellent for the spin–orbit conserving transitions. This is similar to the good agreement seen earlier with the CEPA cross sections,[15] and is not surprising, since the CCSD(T) and CEPA spin–orbit conserving cross sections are nearly the same (Fig. 7).

For transitions in which the spin–orbit manifold changes, the CCSD(T) cross sections, despite being larger than the CEPA values (Fig. 7), are still significantly smaller than the published experimental values. As we have remarked previously,[15] and has been seen experimentally by several groups,[6,9] for transitions from low-$j$ levels of the $\omega=1/2$ spin–orbit manifold into all rotational levels of the $\omega=3/2$ manifold, the cross sections into $\Lambda$-doublet levels of $A''$ reflection symmetry[45,46] will be significantly larger than those for transitions into $\Lambda$-doublet levels of $A'$ reflection symmetry. We see in the lower panel of Fig. 8 that the CCSD(T) inelastic cross sections into levels of $A''$ symmetry

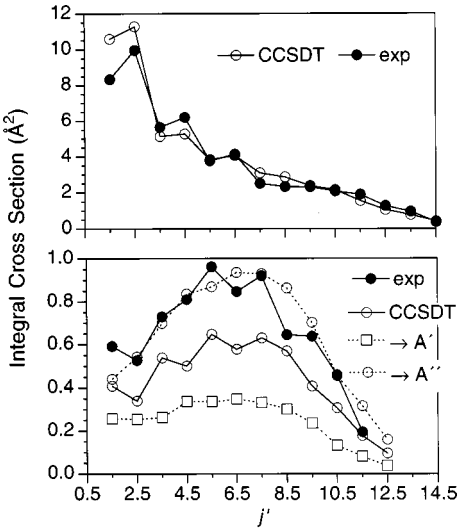


FIG. 8. Comparison of close-coupled, integral cross sections, averaged over initial and summed over final Λ-doublet level [Eq. (12)], for excitation out of the $j=\omega=1/2$ level of NO by collision with Ar; $E_{\mathrm{tot}}=442\ \mathrm{cm}^{-1}$. The filled and empty circles represent, respectively, the experimental results of Joswig *et al.* (Ref. 22) and calculations based on the present CCSD(T) PES's. The upper and lower panels represent, respectively, excitation into rotational levels of the $\omega=1/2(F_1)$ and $\omega=3/2(F_2)$ spin–orbit manifolds. In both cases the experimental values have been scaled so that the sum of the spin–orbit conserving integral cross sections (upper panel) for the transitions shown is equal to the corresponding sum of the theoretical cross sections. In the lower panel the two dashed curves display the cross sections [Eq. (13)] for scattering into the $e(A'')$ and $f(A')$ Λ-doublet levels of the final state.

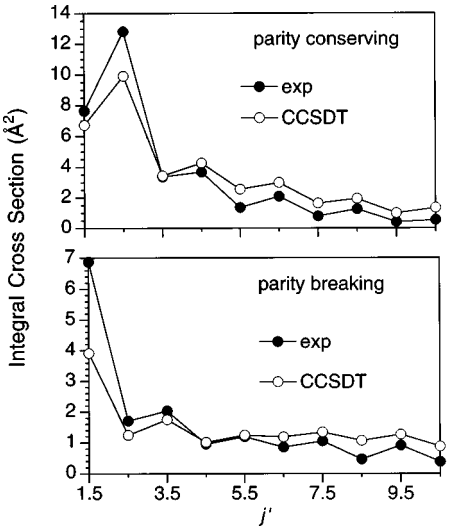


FIG. 9. Comparison of close-coupled, integral cross sections for excitation out of the $j=\omega=1/2,f$ Λ-doublet (negative parity) level of NO by collision with Ar into higher rotational, electronic, Λ-doublet levels of the $\omega=1/2(F_1)$ spin–orbit manifold: $E_{\mathrm{tot}}=442\ \mathrm{cm}^{-1}$. The filled and empty circles represent, respectively, the experimental results of van Leuken *et al.* (Ref. 7) and close-coupled calculations based on the present CCSD(T) PES's. In both cases the experimental values have been scaled so that the sum of the parity breaking and parity conserving integral cross sections for all transitions shown is equal to the corresponding sum of the theoretical cross sections.

agree extremely well with experiment. Unfortunately, Joswig did not report the particular spectral lines which he used to detect the scattered NO molecules,[22,47] so that it is impossible to know whether the good agreement seen in the lower panel of Fig. 8 is real.

In comparison with the experiments of Andresen and co-workers, Stolte and co-workers were able to initially select just the upper $(f,\varepsilon=-1)$ Λ-doublet level of the $j=1/2$ level of NO in their scattering experiments. The cross sections for scattering out of a single Λ-doublet level is expected to show a pronounced oscillatory dependence on the final rotational quantum number.[15]

For collisions involving a molecule in a $^2\Pi$ electronic state, there will be no direct coupling between rotational levels $j$ and $j'$ unless[12,13,43]

$$\varepsilon\varepsilon'(-1)^{j+j'+\lambda}=-1, \tag{14a}$$

where λ is the index in the expansion of the angular dependence of the PES's [Eq. (4)]. As previously stated by van Leuken *et al.*,[7] this condition is equivalent to

$$\varepsilon\varepsilon'(-1)^{\Delta j+\lambda}=1. \tag{14b}$$

As a consequence of the near homonuclear character of the NO molecule, the largest even-λ terms in the expansion of $V_{\mathrm{sum}}$ will be significantly larger in magnitude than the largest of the odd-λ terms. Thus, as discussed in detail by Werner and co-workers in their analysis of their study of inelastic scattering of $\mathrm{OH}(X\,^2\Pi)$,[48] $e/f$ conserving transitions $(\varepsilon'=\varepsilon)$ will be stronger than $e/f$ changing transitions for *even* $\Delta j$, while $e/f$ changing transitions $(\varepsilon'=-\varepsilon)$ will be stronger than $e/f$ conserving transitions for *odd* $\Delta j$. Since the parity of the rotational level is equal to $\varepsilon(-1)^{j-1/2}$, [35] it follows that when even terms dominate in the Legendre expansion of the PES, parity conservation will always be favored over parity change, for all $\Delta j$.

Figure 9 compares the dependence on $j'$ of the CCSD(T) and experimental spin–orbit conserving cross sections out of the $j=\omega=1/2$, $f$ level, again for $E_{\mathrm{tot}}=442\ \mathrm{cm}^{-1}$. As can be seen, the agreement is excellent, both in magnitude and extent of oscillations, although the experimental cross sections are significantly smaller for large $\Delta j$. Because the CEPA and CCSD(T) cross sections are so similar for spin–orbit conserving cross sections at $E_{\mathrm{tot}}=442\ \mathrm{cm}^{-1}$ (see Fig. 7), a similar degree of agreement is seen between experiment and the CEPA cross sections.[7] Figure 10 compares the relative magnitude of the CCSD(T) and experimental cross sections for parity conserving as compared to parity changing transitions. Again, the agreement is excellent, probably within (or close to) the experimental error bars.

Unfortunately, the experiments of Stolte and co-workers were not extended to spin–orbit changing transitions.

Calculations were also carried out at the considerably higher energy $(E_{\mathrm{tot}}=1774\ \mathrm{cm}^{-1})$ used in the recent experiments by McBane and co-workers.[9] At this higher energy, the computational demands of full CC calculations become very high, due to the large number of rotational states which must be included in the expansion of the wave function in Eq. (7). At $E_{\mathrm{tot}}=1774\ \mathrm{cm}^{-1}$, a total of 81 values of the total angular momentum $J$ for each value of the total parity must be included to obtain converged values of the integral cross

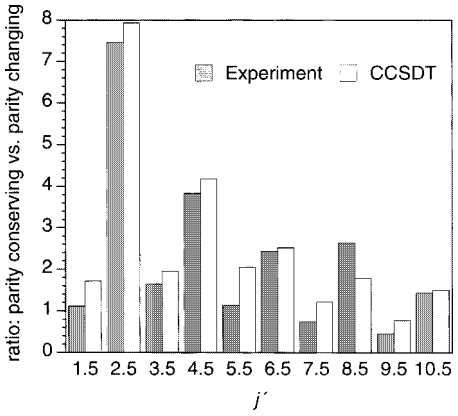


FIG. 10. Ratio of parity conserving to parity breaking integral cross sections for excitation out of the $j=\omega=1/2,f$ $\Lambda$-doublet (negative parity) level of NO by collision with Ar into higher rotational, electronic, $\Lambda$-doublet levels of the $\omega=1/2(F_1)$ spin–orbit manifold; $E_{\rm tot}=442\,{\rm cm}^{-1}$. The filled and empty columns represent, respectively, the experimental results of van Leuken *et al.* (Ref. 7) and calculations based on the present CCSD(T) PES's.

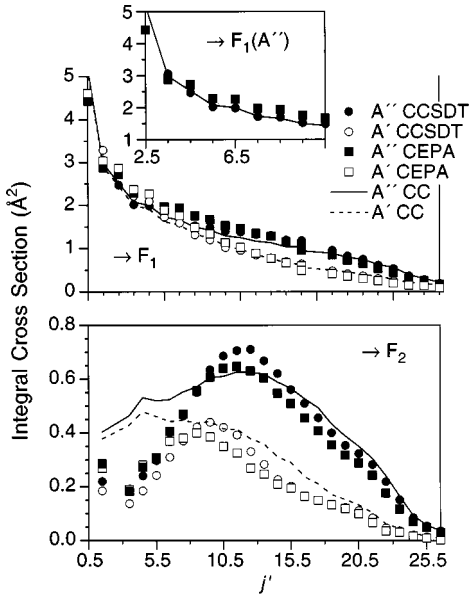


FIG. 11. Comparison of integral excitation cross sections, averaged over initial $\Lambda$-doublet level and averaged over a 4:1 initial population of the $j=1/2$ and $j=3/2$ rotational levels of the NO molecule; $E_{\rm tot}=1774\,{\rm cm}^{-1}$. The open and filled circles refer to coupled-states calculations with the CCSD(T) PES's; the open and filled squares refer to coupled-states calculations with the CEPA PES's (Ref. 15), and the solid and dashed lines refer to close-coupled calculations with the CCSD(T) PES's. The upper and lower panels illustrate, respectively, excitation into rotational levels of the $\omega=1/2(F_1)$ and $\omega=3/2(F_2)$ spin–orbit manifolds. The identification of the reflection symmetry of the final states with the $e/f$ $\Lambda$-doublet labels is discussed in the text and in Ref. 45.

sections [$J=0$ to 320 (Table II) in steps of 4]. Resolution of the CC equations for one value of $J$, and and one value of the total parity, required ~14 hours of cpu time on our fastest workstation (HP J2240). Earlier calculations[9] made use of the computationally faster coupled-states method (CS),[12,49,50] in which use of a body-frame rather than space-frame expansion allows the block diagonalization of the $W(R)$ matrix in Eq. (9).

Figure 11 compares the CS and CC rotational excitation cross sections at $E_{\rm tot}=1774\,{\rm cm}^{-1}$. Since McBane and co-workers[9] reported, separately, cross sections for excitation of the $A'$ and $A''$ $\Lambda$-doublet levels,[45,46] the cross sections displayed correspond to Eq. (13). In the experiments 80% of the NO molecules in the beam are in the $j=\omega=1/2$ level with the remainder in the $j=3/2$, $\omega=1/2$ level, with both $\Lambda$ doublet levels in each rotational level equally populated. Consequently, for the most direct comparison with experiment the theoretical cross sections displayed in Figs. 11–13 reflect this initial average, namely

$$\sigma(j'\omega'\varepsilon';E)=0.8\sigma(j=1/2,\omega=1/2\rightarrow j'\omega'\varepsilon';E)+0.2\sigma(j=3/2,\omega=1/2\rightarrow j'\omega'\varepsilon';E), \tag{15}$$

where $\sigma(j\omega\rightarrow j'\omega'\varepsilon';E)$ is defined by Eq. (13). Strictly speaking, the experimental conditions define the same collision energy for both initial values of $j$, which corresponds to two different total energies ($E_{\rm tot}=1774\,{\rm cm}^{-1}$ and 1779 ${\rm cm}^{-1}$), while the theoretical calculations were carried out at a single total energy ($E_{\rm tot}=1774\,{\rm cm}^{-1}$). We anticipate that this variation of 0.3% in the total energy will lead to a negligible change in the integral cross sections.

In contrast to the results at lower energy (see Fig. 7) we observe an overall excellent degree of agreement between both the coupled-states CCSDT(T) and CEPA cross sections, in particular even for the $\omega=1/2\rightarrow3/2$ transitions. Comparison between the CS and CC cross sections, based on the same CCSD(T) PES's shows good agreement, except for transitions with low $\Delta j$. Although CC calculations are far more costly in computer time, they appear to be necessary for a truly quantitative comparison with experiment. We observe, finally, that excitation into rotational levels of $A''$ reflection symmetry[45,46] is consistently favored, as anticipated in our earlier calculations at lower energy[15] and seen experimentally by Reisler, McBane, and their co-workers.[6,9]

McBane and co-workers scaled their experimental cross sections (see Fig. 5 of Ref. 9) to minimize the overall deviation from the CEPA CS cross sections for excitation into rotational levels of the $\omega=1/2(F_1)$ spin-orbit manifold with $j'\geqslant7.5$. Figure 12 compares the CC cross sections calculated on the CCSD(T) PES's with the scaled experimental values. The overall trends in the experimental values are well reproduced by the calculations, in particular the general propensity to populate rotational levels of $A''$ reflection symmetry. However, we observe that the calculations consistently underestimate the cross sections for excitation into the $F_2$ spin–orbit manifold. Figure 13 compares the CC cross sections with the experimental values, reduced by an additional

TABLE II. Parameters defining ArNO scattering calculations.[a]

| $E_{\rm tot}({\rm cm}^{-1})$ | $J_{\rm max}$[b] | $j_{\rm max}$[c] | $N_{ch}$[d] |
|---|---|---|---|
| 442 | 160.5 | 17.5 | 342 |
| 1774 | 320.5 | 28.5 | 1758 |

[a]See Ref. 44.
[b]Maximum value of the total rotational angular momentum in Eq. (8).
[c]Maximum NO rotational level included in wave function expansion.
[d]Total number of coupled channels.

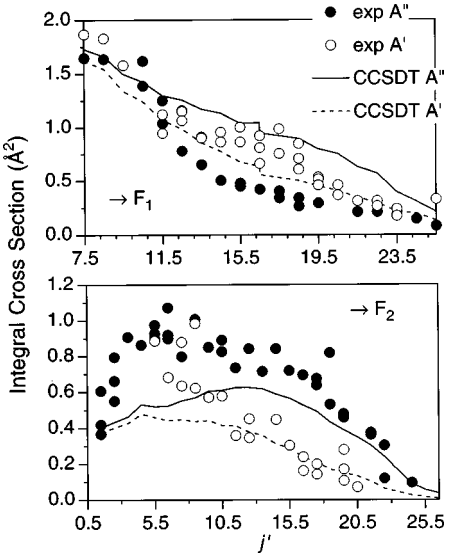


FIG. 12. Comparison of integral excitation cross sections, averaged over initial Λ-doublet level and averaged over a 4:1 initial population of the $j=1/2$ and $j=3/2$ rotational levels of the NO molecule; $E_{tot}=1774\,cm^{-1}$. The open and filled circles refer to the experimental results of McBane and co-workers (Ref. 9) and the solid and dashed lines refer to close-coupled calculations with the CCSD(T) PES's. The upper and lower panels illustrate, respectively, excitation into rotational levels of the $\omega=1/2(F_1)$ and $\omega=3/2(F_2)$ spin–orbit manifolds. The scaling of the experimental results and the identification of the reflection symmetry of the final states with the Λ-doublet labels are discussed in the text and in Ref. 45.

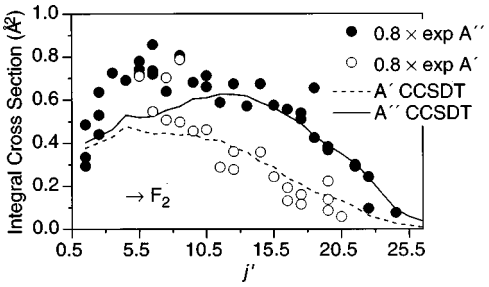


FIG. 13. Comparison of integral excitation cross sections, averaged over initial Λ-doublet level and averaged over a 4:1 initial population of the $j=1/2$ and $j=3/2$ rotational levels of the NO molecule; $E_{tot}=1774\,cm^{-1}$. The open and filled circles refer to the experimental results of McBane and co-workers (Ref. 9) and the solid and dashed lines refer to close-coupled calculations with the CCSD(T) PES's. The cross sections refer to excitation into rotational levels of the $\omega=3/2(F_2)$ spin–orbit manifolds. The experimental cross sections are scaled by a factor of 0.8 from those shown in Fig. 12. The identification of the reflection symmetry of the final states with the Λ-doublet labels is discussed in the text and in Ref. 45.

scaling of 0.8. This figure shows how the calculation reproduces extremely well the relative dependence on $j'$ of the spin–orbit changing transitions as well as the relative $A''$ vs. $A'$ propensity.

## V. DISCUSSION

We have presented here the results of full close-coupling calculations for the scattering of NO by Ar at two energies (442 and 1774 $cm^{-1}$). The calculations were based on new ArNO potential energy surfaces, calculated with a coupled-cluster method [CCSD(T)] including perturbative treatment of triple excitations and using a large atomic orbital basis set, further extrapolated to the complete basis set limit. Although the depth of the van der Waals wells in the two ($A'$ and $A''$) PES's is considerably deeper than that predicted by our earlier CEPA calculations,[15] the topology of the surfaces is remarkably similar.

For rotational excitation within the $\omega=1/2(F_1)$ spin–orbit manifold, calculations at $E=442\,cm^{-1}$ indicate that both the CCSD(T) and CEPA PES's predict similar cross sections. Agreement is excellent, also, with the earlier experimental cross sections from Andresen's group.[5,22] and with more recent experimental results in which the $f$ Λ-doublet level is initially excited.[7] For higher $\Delta j$, the latter experiments predict cross sections which are slightly smaller than calculated. This residual difference might be a reflection of experimental uncertainties. Because the CEPA and CCSD(T) cross sections are so similar, it is hard to see how further improvements in the calculated PES's will reduce this difference.

For spin–orbit changing ($\omega=1/2\rightarrow3/2$) transitions, the CCSD(T) cross sections are somewhat larger than CEPA values. This is likely an indication of a slight contraction of the CCSD(T) average potential ($V_{sum}$), as compared with the CEPA PES's. This permits the collision partners to approach slightly closer, to a region where the difference potential ($V_{dif}$) is slightly larger. For collisions involving a $^2\Pi$ molecule in rotational levels well described by Hund's case (a), $V_{dif}$ is primarily responsible for the coupling between the spin-orbit manifolds.[12] Consequently, larger $V_{dif}$ should lead to larger cross sections for $\omega=1/2\rightarrow3/2$ transitions.

Unfortunately, comparison with experiment.[5,22] for the $\omega=1/2\rightarrow3/2$ transitions at $E=442\,cm^{-1}$, is inconclusive. The calculations indicate that cross sections for transitions into the $F_2$ levels of $\Pi(A'')$ symmetry[46] ($e$-labeled) will be significantly larger than for transitions into the $F_2$ levels of $\Pi(A')$ symmetry. However, no record was retained[47] of which final state Λ-doublet level was probed in the experiments. Until this (or an equivalent) experiment is redone, the ambiguity will persist.

At a total energy of 1774 $cm^{-1}$, the cross sections based on the CEPA and CCSD(T) PES's are extremely similar. This suggests that there will be very little change in the calculated cross sections with increasing refinement of the PES. Comparison with the experimental results of McBane and co-workers[9] reveals substantial differences, particularly for the $\omega=1/2\rightarrow3/2$ transitions.

Thus, despite the sophistication of both the *ab initio* calculations on which the PES's are based and the scattering calculations, substantial differences persist between the calculated inelastic cross sections and those extracted from experiment. In a recent paper[3] we showed that the determination of thermal rate coefficients, particularly at very low temperature, can provide another stringent test of our ability to model collisions of Ar with NO. Further, rate constant measurements provide absolute quantities, which remove another ambiguity in the comparison with theory. We would encourage further experimental study of spin–orbit changing transitions in collisions of NO with Ar, in particular the determination of thermal rate coefficients.

For the ArNO system, as in the interaction of other radicals in $^2\Pi$ electronic states with noble gasses,[51] spectroscopic investigation of the bound states of the complex provides additional information on the shape of the PES's in the region of the van der Waals minimum, information which complements that available from inelastic scattering studies. In a companion paper,[38] we will use the present CCSD(T) PES's to investigate the bound states of the Ar–NO complex, and make a comparison with experiment.

## ACKNOWLEDGMENTS

The author is grateful to the National Science Foundation for support under Grant No. CHE-9971810. He would also like to thank Kirk Peterson for discussions about the complete basis set extrapolation used in Sec. II.

[1] S. D. Jons, J. E. Shirley, M. T. Vonk, C. F. Giese, and W. R. Gentry, J. Chem. Phys. **105**, 5397 (1996).
[2] G. Parlant and M. H. Alexander, J. Chem. Phys. **92**, 2287 (1990).
[3] P. L. James, I. R. Sims, I. W. M. Smith, M. H. Alexander, and M. Yang, J. Chem. Phys. **109**, 3882 (1998).
[4] A. S. Sudbø and M. M. T. Loy, Chem. Phys. Lett. **82**, 135 (1981), J. Chem. Phys. **76**, 2646 (1982)
[5] P. Andresen, H. Joswig, H. Pauly, and R. Schinke, J. Chem. Phys. **77**, 2204 (1982).
[6] C. R. Beiler, A. Sanov, and H. Reisler, Chem. Phys. Lett. **235**, 175 (1995).
[7] J. J. van Leuken, F. H. W. van Amerom, J. Bulthuis, J. G. Snijders, and S. Stolte, J. Phys. Chem. **99**, 15573 (1995).
[8] J. J. van Leuken, J. Bulthuis, S. Stolte, and J. G. Snijders, Chem. Phys. Lett. **260**, 595 (1996).
[9] A. Lin, S. Antonova, A. P. Tsakotellis, and G. C. McBane, J. Phys. Chem. **103**, 1198 (1999).
[10] H. Klar, J. Phys. B **6**, 2139 (1973).
[11] S. Green and R. N. Zare, Chem. Phys. **7**, 62 (1975).
[12] M. H. Alexander, J. Chem. Phys. **76**, 5974 (1982).
[13] M. H. Alexander, Chem. Phys. **92**, 337 (1985).
[14] G. C. Nielson, G. A. Parker, and R. T Pack, J. Chem. Phys. **66**, 1396 (1977).
[15] M. H. Alexander, J. Chem. Phys. **99**, 7725 (1993).
[16] W. Meyer, Int. J. Quantum Chem., Symp. **5**, 341 (1971).
[17] W. Meyer, J. Chem. Phys. **58**, 1017 (1973).
[18] T. Orlikowski and M. H. Alexander, J. Chem. Phys. **79**, 6006 (1983).
[19] T. Orlikowski and M. H. Alexander, J. Chem. Phys. **80**, 4133 (1984).
[20] M. Yang and M. H. Alexander, J. Chem. Phys. **103**, 6973 (1995).
[21] T. Schmelz, P. Rosmus, and M. H. Alexander, J. Phys. Chem. **98**, 1073 (1994).
[22] H. Joswig, P. Andresen, and R. Schinke, J. Chem. Phys. **85**, 1904 (1986).
[23] P. J. Knowles, C. Hampel, and H.-J. Werner, J. Chem. Phys. **99**, 5219 (1993).
[24] W. Meyer, Theor. Chim. Acta **35**, 277 (1974).
[25] T. H. Dunning, Jr., J. Chem. Phys. **90**, 1007 (1989).
[26] R. A. Kendall, T. H. Dunning, Jr., and R. J. Harrison, J. Chem. Phys. **96**, 6796 (1992).
[27] D. E. Woon and T. H. Dunning, Jr., J. Chem. Phys. **98**, 1358 (1993).
[28] K. P. Huber and G. Herzberg, *Molecular Spectra and Molecular Structure. IV. Constants of Diatomic Molecules* (Van Nostrand Reinhold, New York, 1979).
[29] S. F. Boys and F. Benardi, Mol. Phys. **19**, 553 (1970).
[30] P. D. A. Mills, C. M. Western, and B. J. Howard, J. Phys. Chem. **90**, 4961 (1986).
[31] K. A. Peterson and T. H. Dunning, Jr., J. Phys. Chem. **101**, 6280 (1997).
[32] D. M. Brink and G. R. Satchler, *Angular Momentum*, 2nd ed. (Clarendon, Oxford, 1968).
[33] A FORTRAN program to determine the radial expansion coefficients $V_\lambda(R)$ in the expansion of the modified $V_{\rm sum}$ and $V_{\rm dif}$ as a function of $R$ are available on request from the author by electronic mail (address: millard_*h*_alexander@umail.umd.edu). Please supply a return electronic mail address.
[34] H. Lefebvre-Brion and R. W. Field, *Perturbations in the Spectra of Diatomic Molecules* (Academic, New York, 1986).
[35] J. M. Brown, J. T. Hougen, K.-P. Huber, J. W. C. Johns, I. Kopp, H. Lefebvre-Brion, A. J. Merer, D. A. Ramsay, J. Rostas, and R. N. Zare, J. Mol. Spectrosc. **55**, 500 (1975).
[36] M.-L. Dubernet, D. Flower, and J. M. Hutson, J. Chem. Phys. **94**, 7602 (1991).
[37] W. H. Green, Jr. and M. I. Lester, J. Chem. Phys. **96**, 2573 (1992).
[38] M. H. Alexander, J. Chem. Phys. **111**, 7435 (1999), following paper.
[39] J. T. Hougen, Natl. Bur. Stand. (U. S.) Monogr. 115 (1970).
[40] R. N. Zare, A. L. Schmeltekopf, W. J. Harrop, and D. L. Albritton, J. Mol. Spectrosc. **46**, 37 (1973).
[41] G. Herzberg, *Spectra of Diatomic Molecules*, 2nd ed. (Van Nostrand, Princeton, 1968).
[42] R. N. Zare, *Angular Momentum* (Wiley, New York, 1988).
[43] G. C. Corey and M. H. Alexander, J. Chem. Phys. **85**, 5652 (1986).
[44] HIBRIDON is a package of programs for the time-independent quantum treatment of inelastic collisions and photodissociation written by M. H. Alexander, D. E. Manolopoulos, H.-J. Werner, and B. Follmeg, with contributions by P. F. Vohralik, D. Lemoine, G. Corey, B. Johnson, T. Orlikowski, W. Kearney, A. Berning, A. Degli-Esposti, C. Rist, and P. Dagdigian. More information and/or a copy of the code can be obtained from the website http://www-mha.umd.edu/~mha/hibridon.
[45] M. H. Alexander and P. J. Dagdigian, J. Chem. Phys. **80**, 4325 (1984).
[46] M. H. Alexander *et al.*, J. Chem. Phys. **89**, 1749 (1988).
[47] H. Joswig, *Messungen integraler Zustandsspezifischer Querschnitte bei Inelastichen NO-Edelgas-Stößen*, Ph.D. thesis, Universität Göttingen, 1983.
[48] A. Degli-Esposti, A. Berning, and H.-J. Werner, J. Chem. Phys. **103**, 2067 (1995), and references contained therein.
[49] P. McGuire and D. J. Kouri, J. Chem. Phys. **60**, 2488 (1974).
[50] D. J. Kouri, in *Atom-Molecule Collision Theory: A Guide for the Experimentalist*, edited by R. B. Bernstein (Plenum, New York, 1979), p. 301.
[51] For a good review, see M. C. Heaven, J. Phys. Chem. **97**, 8567 (1993).